

# Hurst Exponent on the Study of Electrochemical Noise Measurements

J.M. Sánchez-Amaya,<sup>†\*</sup> F.J. Botana,<sup>\*</sup> and M. Bethencourt<sup>\*</sup>

## ABSTRACT

*In this study, an analysis has been made of electrochemical noise (EN) signals of potential and current obtained on immersing samples of the Alloy AA5083 (UNS A95083) in solutions of sodium chloride (NaCl). These signals have been processed using the calculation of the Hurst exponent, a tool derived from the theory of chaos that allows one to estimate the influence that events occurring in the past have on the appearance of new events at subsequent times. However, the classic Hurst exponent was seen to have some limitations for the study of complex signals. In addition, a new Hurst exponent has been proposed for a better interpretation of EN data. The results obtained have enabled the values of the Hurst exponent to be correlated with the predominant mechanism of corrosion.*

**KEY WORDS:** aluminum, chaos, electrochemical noise, Hurst exponent, localized corrosion, rescaled range analysis, transients

## INTRODUCTION

The measurement of electrochemical noise (EN) is a technique that has been used successfully for the study of the behavior of diverse metallic materials subjected to different types of corrosion. As is known, success in the application of this technique is largely determined by the validity of the mathematical

method used in the analysis of the data. Several different methods of analysis have been described in the references, such as the use of statistical parameters, analysis in the frequency domain, tools derived from the transformation of wavelets, or methods based on chaos theory. In accordance with different theories of chaos, the calculation of the so-called Hurst exponent (H) permits the quantification of the degree of autocorrelation existing between the elements that form a data series, and the determination of the influence that events occurring in the past have on the emergence of future events. This exponent was utilized for the first time by Hurst for the study of hydrological data, with the objective of designing a dam on the river Nile.<sup>1-3</sup> Later, thanks to the work of Mandelbrot and Wallis,<sup>4-5</sup> this mathematical tool has been successfully applied in many scientific fields.

As examples of the great versatility presented by this methodology, one can cite its use for analyzing solar activity,<sup>6-7</sup> for monitoring the evolution of the price of electricity,<sup>8</sup> for studying stock market fluctuations,<sup>9</sup> as well as its use in the field of particle physics<sup>10</sup> and in the studies of mechanical sliding in solids.<sup>11</sup>

In the bibliography,<sup>12</sup> one of the ways in which the H exponent can be useful is to detect changes in the persistence of a data series. From a theoretical point of view, values of  $H = 0.5$  would indicate that the series analyzed is random; in other words, each event included in the series is independent of the other. On the other hand, if  $0.5 < H < 1$ , the series analyzed is said to be persistent; in other words, the events that appear in the series are related. Thus, in this type of series, the emergence of one event would

Submitted for publication April 2004; in revised form, March 2005. Presented as paper no. 04767 at CORROSION/2004, March 2004, New Orleans, LA.

<sup>†</sup> Corresponding author. E-mail: josemaria.sanchez@uca.es.

<sup>\*</sup> University of Cádiz, Avda. Republic Saharaui s/n, Apdo 40, Puerto Real, E-11510, Cádiz, Spain.

Promote the initiation of the following one. However, if  $0 < H < 0.5$ , the series is antipersistent. It is a characteristic of this latter type of series that the emergence of one event delays or inhibits the initiation of a new event in the series.<sup>12</sup>

As a consequence of its great versatility, the Hurst exponent has also been used for the study of corrosion processes. Thus, the utilization of  $H$  as a parameter for evaluating the morphology of the pits generated in localized corrosion processes has been proposed.<sup>13</sup> Similarly it has been used in the analysis of data obtained by means of EN measurement. Others<sup>14-15</sup> have proposed the use of  $H$  for evaluating the protective properties of organic coatings. More specifically, Moon and Skerry<sup>14</sup> postulate the existence of a linear relationship between the values of  $H$ , calculated from EN records, and the resistance to corrosion of the paints studied. In another study, Greisiger and Schauer<sup>15</sup> utilized the Hurst exponent to obtain information on the mechanism of corrosion processes.

However, as it occurs with other mathematical tools utilized for the analysis of EN data, the relationship between the values of  $H$  and the predominant mechanism of corrosion appears to depend on the system studied. Thus, for example, in the study of coated steels by Greisiger and Schauer,<sup>15</sup> EN signals are obtained that give rise to values of  $H < 0.5$ . These values are associated with the existence of protective coatings. In contrast, values of  $H > 0.5$  are associated with situations in which a loss of the protective power of the coatings is produced. In accordance with these results,<sup>15</sup> the calculation of  $H$  is proposed to monitor the evolution of coatings and to detect when they lose their protective properties.

Recently, Horváth and Schiller<sup>12</sup> have applied the method of Hurst to the analysis of potential signals obtained from samples of 99.99% pure aluminum in different corrosive media. In particular, they studied the influence of the presence of chlorides on the behavior of the metal in slightly acidic media. Thus, in the absence of chlorides, values of  $H$  ranging between 0.7 and 0.8 are obtained. However, in the presence of chlorides, the  $H$  values depend on the temporal interval in which this exponent is calculated. So, the formation of pits is associated with values of  $H$  ranging from 0.1 to 0.3, provided  $H$  is measured at intervals of time longer than the lifetime of a pit. Nevertheless,  $H$  was observed to be higher than 0.5 when this parameter is estimated in intervals lower than the lifetime of pits. Horváth and Schiller<sup>12</sup> proposed that the period of time when the change from persistence to antipersistence (crossover time) is a good estimator of the lifetime of the pits in some systems. Horváth's study demonstrates the potential usefulness of  $H$  for detecting changes in the corrosive behavior of a system.

<sup>(1)</sup> UNS numbers are listed in *Metals and Alloys in the Unified Numbering System*, published by the Society of Automotive Engineers (SAE International) and cosponsored by ASTM International.

However, current signals are not analyzed nor are the corrosion mechanisms that give rise to persistent signals studied in depth in that article.<sup>12</sup>

One of the methodologies most frequently used for the calculation of the Hurst exponent is the method of rescaled range analysis, also known as the R/S method. A detailed description of this method is given elsewhere.<sup>12</sup> However, in the present study, we have included a part describing in summary form the basic steps to apply this method of calculation. This method considers a linear relationship between  $\log R/S$  values and  $\log \tau$ , whose slope is  $H$  (the calculation and interpretation of  $R/S$  and  $\tau$  values is detailed in the "R/S Method" section). After this section, some simulated signals were analyzed using this method. Additionally, the experimental devices used to obtain the EN signals are described. Later, the results are presented and discussed corresponding to the calculation of the Hurst exponent for analyzing EN signals, of current and potential, obtained from the immersion of AA5083 (UNS A95083)<sup>(1)</sup> samples in solutions of sodium chloride (NaCl). The results obtained showed that most simulated and experimental signals did not give  $R/S$  values proportional to  $\tau^H$ , that is, the slope of  $\log R/S$  vs.  $\log \tau$  was seen to depend on the  $\tau$  values taken for the estimation of  $H$ . In the present paper, a new method is proposed to solve this limitation, consisting of calculating the Hurst exponent for each  $\tau$  value. Finally, the results obtained from analyzing AA5083 in NaCl enabled values of the Hurst exponent to be correlated with the mechanism of corrosion predominant at each moment during the assay.

### R/S Method

We shall consider the time series  $x_i$  of  $i$  points, where  $i = 0, 1, \dots, N$ . The  $(N+1)$  points of the series are separated by a time interval,  $\Delta t$ , such that the total duration of the series is  $T = (N+1) \times \Delta t$ . In the R/S method, a division of the records in time intervals of  $j$  points, termed intervals of analysis or time lags, is initially performed. So, the length of these time lags are  $\tau = j \times \Delta t$  ( $j < N$ ).

The mean value of  $x_i$  in the intervals of analysis is calculated using the expression:

$$\bar{x}_j = \frac{1}{j} \sum_{i=1}^j x_i \quad (1)$$

In addition, the accumulative deviation of the data with respect to the mean, in the time lag, can be defined as:

$$y_{j,k} = \sum_{i=1}^k (x_i - \bar{x}_j) \quad (2)$$

where  $k$  takes all the integer values that meet the condition:  $1 \leq k \leq j$ . As can be deduced from this expression,  $y_{j,k}$  is a vector whose values accumulate the

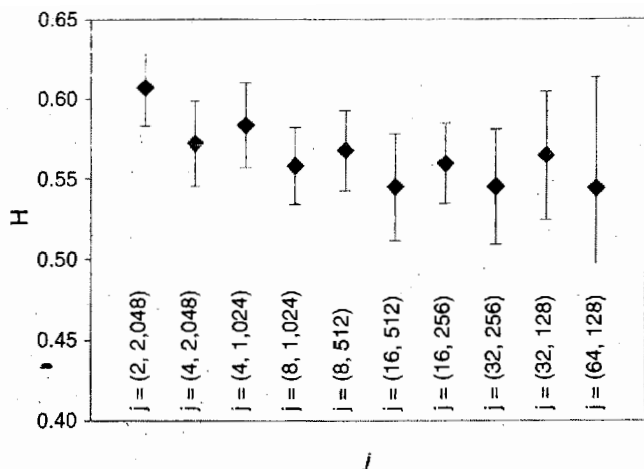


**FIGURE 1.** Mean and standard deviations of the values of  $H$  of random series of 2,048 points, in function with the scale of analysis ( $j$ ).

differences between  $x_i$  and the mean in the interval of analysis ( $\bar{x}_j$ ), from  $x_i$  up to  $x_k$ , as indicated by the name given to this parameter (accumulative deviation). Subsequently, the range ( $R_j$ ) is calculated. This is the difference between the maximum and minimum values of the accumulative deviation ( $y_{j,k}$ ) of the  $j$  points of the time lag:

$$R_j = \max y_{j,k} - \min y_{j,k} \quad (3)$$

The standard deviation of  $x_i$  in the period of time,  $\tau$ , will be given by:

$$S_j = \sqrt{\frac{1}{j} \sum_{i=1}^j (x_i - \bar{x}_j)^2} \quad (4)$$

Having calculated the range ( $R_j$ ) and the standard deviation ( $S_j$ ) in the period of time  $\tau$ , it is possible to define the rescaled range of  $x_i$  in this time period of  $j$  points:  $R_j/S_j$ . As commented previously, the record comprises  $N$  points, which can be divided into  $N/j$  consecutive intervals of length  $j$ , without overlapping. So, the intervals are constructed maintaining  $j$  constant, being  $m$  the number of the interval, where  $m = 1, 2, 3, \dots, N/j$ . Once these  $N/j$  intervals of time period  $\tau$  have been defined, the rescaled range of each interval can be calculated using the procedure described. Taking the mean of the  $N/j$  values of  $R_{m,j}/S_{m,j}$  of all the intervals of  $j$  points, we obtain the mean adjusted range of the time period  $\tau$ :

$$R/S = \frac{1}{(N/j)} \sum_{m=1}^{N/j} (R_{m,j}/S_{m,j}) \quad (5)$$

Subsequently, we can calculate different values of  $R/S$  of the series  $x_i$ , varying the number of points ( $j$ ) of

the intervals of analysis in such a way that different values of  $R/S$  may be obtained in function of  $\tau$ , since  $\tau = j \times \Delta t$ .

It has been observed experimentally that for very many natural phenomena, a relationship exists between  $R/S$  and  $\tau$ :

$$(R/S) \propto \tau^H \quad (6)$$

where  $H$  is the Hurst exponent. This exponent usually takes a value between 0 and 1.

The estimation of the Hurst exponent is normally performed by means of the graphic representation of  $\log(R/S)$  against  $\log(j)$ , the slope of which directly provides  $H$ . It should be pointed out that the extreme values of  $\tau$  are not usually taken into account for the calculation of  $H$ . On the one hand, if the values of  $\tau$  for calculating  $H$  are very low (for example,  $\tau = 2\Delta t$  or  $4\Delta t$ ), a large number of values of  $R/S$  are averaged ( $N/2$  or  $N/4$ , respectively), but these values present a very wide dispersion. This high degree of dispersion occurs because only a few values of the signal ( $2\Delta t$  or  $4\Delta t$  in the example) are utilized in the calculation of each value of  $R/S$ . On the other hand, if  $\tau$  is very large (for instance,  $\tau = N\Delta t$  or  $N\Delta t/2$ ), very few values of  $R/S$  are averaged (1 or 2, respectively), since the intervals of analysis are very large; therefore, these values cannot be considered representative of the series. Consequently, the values of  $j$  that are chosen for the calculation of  $H$  should be neither very high nor excessively low.<sup>12</sup>

With the objective of verifying the validity of the algorithm used for calculating  $H$ , several different numerical series have been simulated with a computer. Thus, a set of simulated series with different degrees of persistence/antipersistence has been studied by means of the  $R/S$  method in the following section.

## SIMULATED SIGNALS

In this study, a different series with 2,048 points ( $N = 2^{11}$ ) have been simulated, with the objective of verifying the validity of the algorithm used to calculate  $H$ . Initially, a random series has been simulated, where the optimum range of  $j$  for the calculation of  $H$  has been studied. Later, a random series of higher  $N$  was processed to see the influence of  $N$  in the estimation of  $H$ . Subsequently, different persistent and antipersistent series have been simulated, where the influence of the degree of persistence or antipersistence on the  $H$  of the series has been studied. Other types of signals that have been studied include those formed by transients, as well as linear combinations of transients, with sinusoidal signals.

In a first study, a random series of 2,048 points was simulated, to determine the optimum values that  $j$  should take for estimating  $H$  (using the  $R/S$  method). The random numbers of this series were generated in

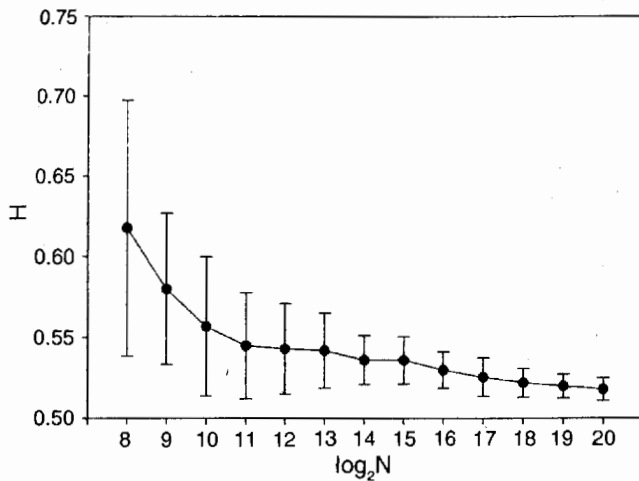


FIGURE 2. Influence of  $N$  in the estimation of  $H$  in random signals.

the (0,1) range. In Figure 1 the influence of the values of  $j$  on the values of  $H$  obtained can be observed.

It can be observed that the values of  $H$  depend strongly on the range of  $j$  values that we analyze. Thus, if very small or very large values of  $j$  are taken ( $j = 2, 4, 1,024, \text{ or } 2,048$ ), the values of  $H$  obtained for random signals are very high. This tendency has also been observed by Horváth and Schiller.<sup>12</sup> On the other hand, if the range of  $j$  is excessively small ( $j \in [64, 128]$ ), the values of  $H$  show a wide spread, since few values are used in the calculation of  $H$ . The authors of this study consider that  $j \in (16, 512)$  is the range that provides the values of  $H$  closest to 0.5 for signals of 2,048 points, without having too great a dispersion ( $H = 0.545 \pm 0.033$ ). In general, the values obtained for  $H$  are larger than the theoretical value of 0.5. The reason for this behavior may be that the signals studied here are finite, while the theoretical value of  $H = 0.5$  would be obtained in infinite random signals. This assumption has been tested by means of processing a random series higher than 2,048 points. In Figure 2,  $H$  values in the range  $j \in (16, N/4)$  have been estimated. The figure shows that the higher  $N$  is in random signals, the closer their  $H$  values are to the theoretical value of 0.5.

In continuation, we present the results obtained in the analysis of a persistent series generated, in other words, comprising data influenced by the preceding values ( $x_i$ ). The introduction of dependence in the data of these new series is achieved by the application of the algorithm:

$$x_i^p = 2(x_i^p - 0.5); x_i^p = wx_{i-1}^p + (1-w)x_i \quad (7)$$

where  $x_i$  is the series composed of random numbers falling in the range (0,1),  $x_i^p$  is the persistent series generated by numbers falling in the range (0,1),  $x_i^p \in (-1, 1)$ , and  $w$  is the degree of persistence of  $x_i^p$ .  $w \in [0, 1]$  and fixes the correlation between the data of the

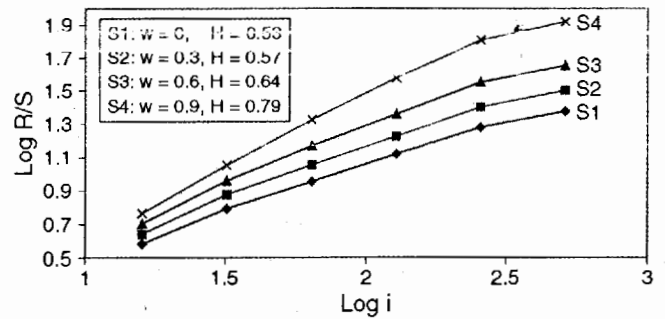


FIGURE 3. Values of  $\log R/S$  vs.  $\log j$  of simulated signals with different degrees of persistence ( $w$ ).

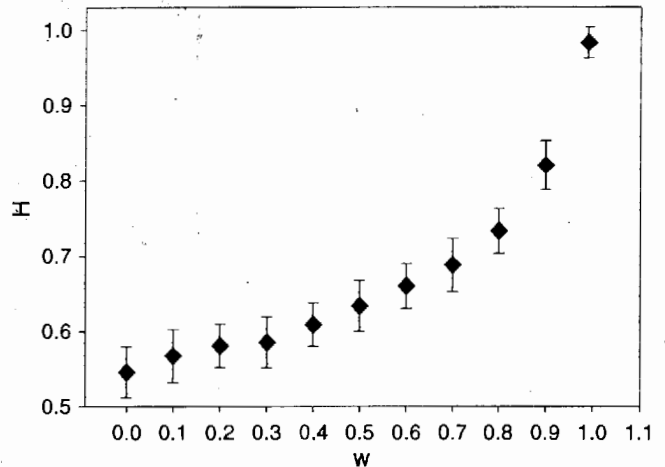


FIGURE 4. Values of  $H$  obtained in a simulated series with different degrees of persistence.

numerical series generated;  $w$  defines the persistence of the signal. Figure 3 includes the values of  $\log R/S$  against  $\log \tau$  ( $j \in [16, 512]$ ) of signals obtained from the same  $x_i$ , where the value of  $w$  has been modified. In this Figure 3, it can be observed that the series generated with a larger  $w$  are those that have a larger slope, and therefore are those that have a larger Hurst exponent. In Figure 4, the mean values and values of the standard deviation of  $H$  obtained for the persistent series of  $w = 0, 0.1, 0.2, \dots, 0.9, \text{ and } 0.99$  are represented. For each  $w$ , the mean and the standard deviation of 50 simulated series have been estimated. In this Figure 4, it can be observed that  $H$  increases gradually as  $w$  increases. However, if  $w > 0.8$ ,  $H$  increases more rapidly with  $w$ , until  $w = 0.99$  is reached, giving a value of  $H$  close to 1. On analyzing the standard deviation of the values of  $H$ , it can be deduced that the dispersion of the data is similar in the entire range of  $w$ , except for  $w = 0.99$ , where the standard deviation is lower. This Figure 4 shows that the R/S method distinguishes signals with different degrees of persistence.

In Reference 12, antipersistent signals were designed. In this type of signal, it is observed that there

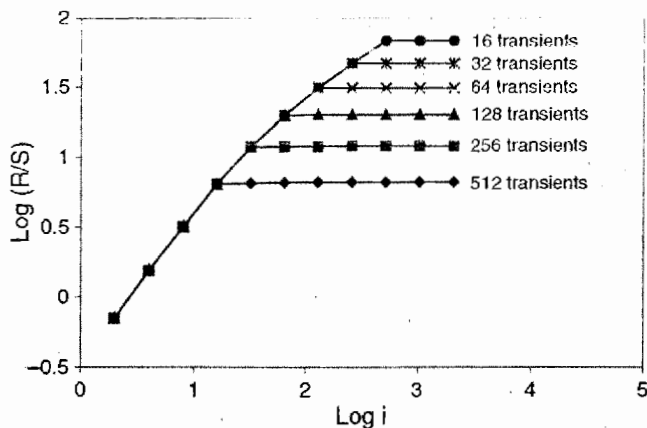


FIGURE 5. Values of  $\log R/S$  vs.  $\log j$  of a series composed of the numbers of transients equally spaced and with the same amplitude.

is a change of slope in the representation of  $\log R/S$  vs.  $\log \tau$ . This change of slope takes place at a specific  $\tau$ , known as the crossover time or  $\tau_c$ . Thus, if  $\tau$  is less than  $\tau_c$ ,  $H > 0.5$ , while if  $\tau > \tau_c$ ,  $H < 0.5$ .  $\tau_c$  is related to a change from persistence to antipersistence in the signal.

Presented next are the results obtained by analyzing, using the R/S method, simulated signals composed of different numbers of transients ( $x_i^{T1}$ ). These transients consisted of a rapid increase in the values of the signal, followed by an exponential type of decline in the values of the series. Five different kinds of signals based on transients were simulated and studied with the R/S method: signals with transients equally spaced ( $x_i^{T1}$ ), signals with transients equally spaced but with different amplitudes ( $x_i^{T2}$ ), signals with different spaces between transients ( $x_i$ ) and a linear combination of a random signal, and a transient-based signal ( $x_i^{T4}$ ). These latter signals have been recently studied through different methods designed to obtain their Hurst exponent, with the R/S method being the one that gave better results.<sup>16</sup> The last kind of signals ( $x_i^{T5}$ ) were composed by transients and a sinusoidal signal.

Represented in Figure 5 are the values of  $\text{Log } R/S$  vs.  $\text{Log } j$  of the series composed of different numbers of transients ( $x_i^{T1}$ ). The number of transients ( $N_T$ ) has been indicated in the figure. In Figure 5, it can be observed that there is a change in the slope in these series. In these signals,  $\tau_c$  coincides with the separation between transients;  $\tau_c = N/N_T$ . This indicates that these series are persistent if the range of  $j$  measured is lower than  $\tau_c$ , while they are antipersistent if the range of  $j$  is greater than  $\tau_c$ . Note in Figure 5 that the slope of the curves after  $\tau_c$  is zero ( $H = 0$ ), since the amplitudes of the transients in these signals are equal, and therefore,  $R/S$  values for  $j > \tau_c$  are also equal. However, the experimental data do not usually present these exact constant time intervals between transients with the same amplitude. Figures 6

through 9 show more realistic signals to be compared with that obtained from the EN data of AA5083 in chloride solutions.

Figure 6 shows the  $R/S$  values of the second kind of transient-based signals ( $x_i^{T2}$ ). The amplitudes of each transient are the sum of an imposed number plus a random number. The coefficient " $A_1$ " marks the weight of the amplitudes imposed to the random amplitudes of transients. In this case,  $A_1 = 0$  would mean that amplitudes are purely random between 0 and 1; while if  $A_1 = 10$ , the amplitudes would oscillate between 10 and 11. It can be seen in this figure that antipersistence can only be achieved when  $A_1 > 1$ , since values lower than 1 lead to  $H$  values higher than 0.5.

Figure 7 shows the  $R/S$  values of the signals with variable intervals between transients,  $x_i^{T3}$ .  $\text{StDv}$  is the standard deviation of the space between transients;  $\text{StDv}$  marks the variability of the interval sizes. The figure clearly shows that the higher the  $\text{StDv}$ , the higher  $H$  is, reaching values of random signals ( $H = 0.57$ ), when  $\text{StDv} = 10$ .

In Figure 8, the  $R/S$  values of signals composed of a combination of transients and a random signal ( $x_i^{T4}$ ) have been plotted. In this case,  $A_2$  marks the weight of the transient signal over the random signal, which oscillates between 0 and 1. In this figure, it can be appreciated that  $H$  is fixed by the more weighted component of the signal. So, when  $A_2$  is high,  $x_i^{T4}$  is mainly a transients signal, and  $H$  is low. On the contrary, when  $A_2$  is low,  $x_i^{T4}$  is dominated by the random signal, and  $H$  is close to 0.55.

Lastly, in this study, linear combinations of signals formed by transients and sinusoidal signals have been generated. The analysis of this type of signal will help us later in the analysis of signals coming from chemical systems, since some of these signals show two  $\tau_c$  behavior seen in some experimental signals. These signals were generated by the following algorithm:

$$x_i^{T+S} = x_i^T + A_3 \sin(2\pi i / L) \quad (8)$$

where  $x_i^T$  is the signal formed by transients that was described previously,  $A_3$  is the amplitude of the sine function, and  $L$  is the wavelength of the sine function.

In Figure 9, the values of  $\text{Log } R/S$  vs.  $\text{Log } \tau$  of series  $x_i^{T+S}$  with different values of  $A_3$  are represented. The values taken in this figure were  $N/N_T = 256$ ,  $L = 16$ , and the values of  $A_3$  are indicated in the figure. As can be deduced from Equation (8), the greater the value of  $A_3$ , the greater the weight of the sinusoidal series against the series formed by transients. In Figure 6 it can be observed that if the sinusoidal component has a weight much greater than that formed by transients ( $A_3 = 100$ ), in the representation of the  $\text{Log } R/S$ , only a change in the slope in  $\tau = 16\Delta t$  is observed. This indicates that in this signal,  $\tau_c = 16\Delta t$ , reflecting the period of the wavelength of the sine sig-

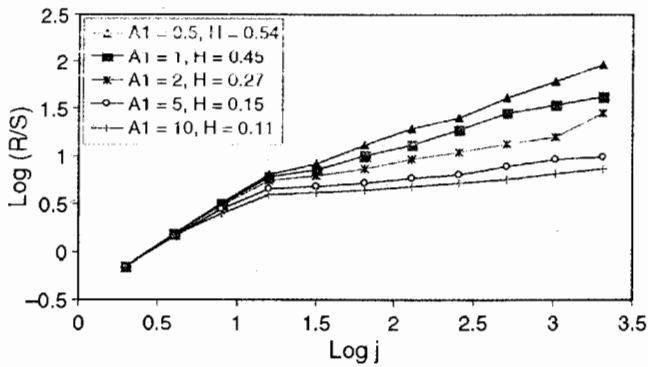


**FIGURE 6.** Values of  $\log R/S$  vs.  $\log j$  of a series composed of transients equally spaced and with different amplitudes.  $A_1$  marks the weight of the imposed amplitudes vs. the random amplitudes of transients.

nal ( $L$ ). In contrast, if the weight of the sine function is very low or zero ( $A_3 = 0.1$  or  $A_3 = 0$ ), the change of slope takes place at  $\tau = N/N_T$ , as previously described in the analysis of signals formed by transients. In this same Figure 6, it can be observed that in the cases where the sine function and that formed by transients have comparable amplitudes ( $A_3$  between 0.1 and 10), two changes of slope exist,  $\tau_{c,1} = 16\Delta t$  and  $\tau_{c,2} = 256\Delta t$ . As can be deduced, in this case,  $\tau_{c,1}$  is due to the sinusoidal signal ( $\tau_{c,1} = L$ ), whereas  $\tau_{c,2}$  is related to the signal formed by transients ( $\tau_{c,2} = N/N_T$ ). Therefore, each  $\tau_c$  revealed the constant time of each signal: In the sine function,  $\tau_c$  is related to the wavelength, while  $\tau_c$  in the transients is related to the space between them. Similarly to the simulated signals, the real signals can have two  $\tau_c$ , revealing the existence of two mechanisms (with different time constants). This is the case of some current noise signals, which will be studied later.

In the analysis of the antipersistent signals that have been generated ( $x_t^A$ ,  $x_t^T$ , and  $x_t^{T+S}$ ), it has been possible to check that there is at least one change in the slope of  $\log R/S$  vs.  $\log \tau$ . This characteristic indicates that, in these signals, the Hurst exponent cannot be calculated with precision by means of the slope of  $\log R/S$  vs.  $\log \tau$  in the range of  $j \in (16, 512)$ . It should be remembered that this range of  $j$  is the optimum for the calculation of  $H$  in random series. In this paper, we propose the use of a new parameter for the analysis of complex signals, such as those previously described ( $x_t^{T+S}$ ). This new parameter ( $H_m$ ), analogous to the classic Hurst exponent, calculates the slope of the straight line tangent to the curve at each point  $m$ :

$$H_m = \frac{(\log R/S)_{2m} - (\log R/S)_{m/2}}{(\log \tau)_{2m} - (\log \tau)_{m/2}} \quad (9)$$

where  $m = 2^p$ , being  $p = 2, 3, \dots, \log_2(N/2)$ .

The analyzed series have  $N = 211$  points, so there are nine possible values of  $m$ : 4, 8, 16, 32, 64, 128,

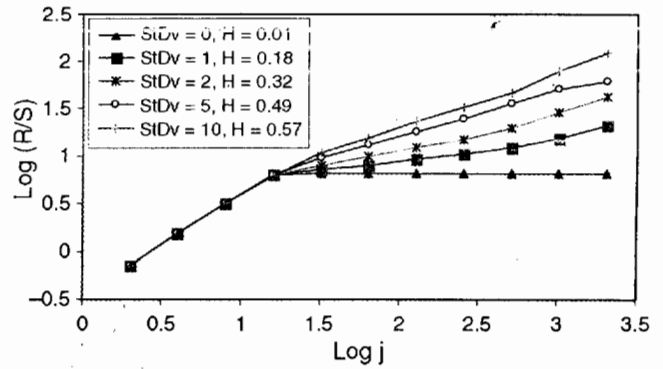


**FIGURE 7.** Values of  $\log R/S$  vs.  $\log j$  of a series composed of transients with different intervals.

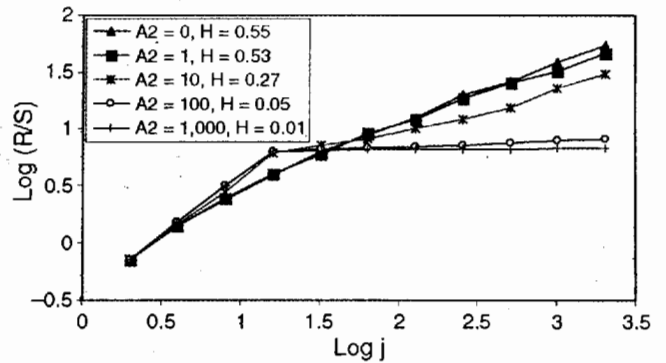


**FIGURE 8.** Values of  $\log R/S$  vs.  $\log j$  of a series composed of transients and a superimposed random signal. In this case,  $A_2$  marks the weight of the transients over the random signal.

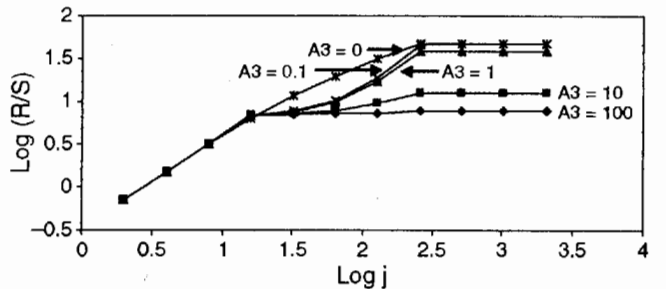


**FIGURE 9.** Values of  $\log R/S$  vs.  $\log j$  of linear combinations of signals formed by transients and sinusoidal signals.

256, 512, and 1,024, defined by means of the nine values of  $p$ : 2, 3, ..., 10. So, in these series of 2,048 points, nine values of  $H_m(p)$  can be obtained.

In Figure 10,  $H_m(p)$  values of the same signals analyzed in Figure 9 have been plotted. In these kinds of representations, the zones where the signals show persistence or antipersistence in the function of  $\tau$  can be observed. In addition, this representation also allows one to know  $\tau_c$ , because this parameter can be estimated by taking the first value of  $p$  whose  $H_m$  is lower than 0.5. In the case of analyzing signals with

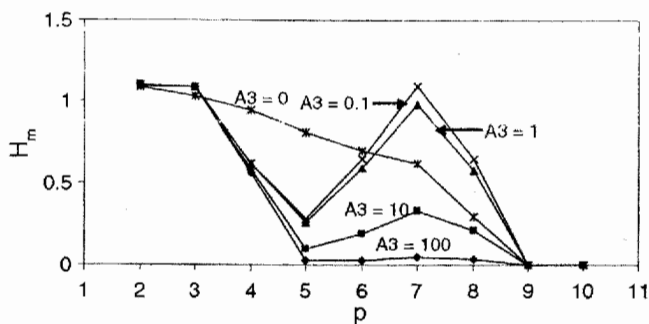


FIGURE 10. Values of  $H_m$  vs.  $p$  of the same signals analyzed in Figure 9.

more than one  $\tau_c$  (like  $x_i^{T+S}$  with  $A_3 = 1$  plotted in Figure 9), it is also possible to calculate these  $\tau_c$ , since the  $\tau_c$  values are all the  $\tau$  values where the two following conditions could be satisfied:  $H_m(p) < 0.5$  and  $H_m(p-1) > 0.5$ . For instance, in the signal of Figure 10 whose  $A_3 = 1$ ,  $\tau_{c,1} = 32$ , and  $\tau_{c,2} = 512$ .

## EXPERIMENTAL SIGNALS

In the present study, the R/S method has been used to analyze the EN records obtained in studying the behavior of AA5083 in solutions of 0.6 M NaCl in the function of exposure time. The EN measurements were taken using a cell configuration with two identical electrodes formed by two cylindrical samples of 1 cm<sup>2</sup> area, protected on their lateral surface with a coating to minimize crevice corrosion.<sup>17</sup> Before the assay, the electrodes were polished to 1,200 grit and cleaned with distilled water. A silver/silver chloride (Ag/AgCl) electrode was used as the reference electrode. The cell used is described in detail elsewhere.<sup>18</sup>

The  $H$  of the  $E$  and  $I$  records was obtained by analyzing the differences in the signals, since it is the fluctuations in the signal and not their absolute values that provides the information. This way of analyzing the experimental signals has already been used by Horváth and Schiller.<sup>12</sup> This methodology is found to detect easily fast fluctuations of the signals, like transients, since it removes the drift from the data. Thus, the signals analyzed were:

$$x_i = \Delta E_{i+1} - \Delta E_i \text{ and } x_i = \Delta I_{i+1} - \Delta I_i, \quad i = 1, 2, \dots, N \quad (10)$$

In each record of EN, a total of 2,048 points were taken at a sampling velocity of 2.15 points per second; therefore, the time of each record was approximately 15 min. In this study, 10 consecutive records were measured in each interval of 10 h, with the objective of averaging the values of the Hurst exponent in these consecutive measurements. The signals of potential and current were measured simultaneously

using a Solartron 1287<sup>†</sup> potentiostat controlled by the Corrware<sup>†</sup> program.

## RESULTS

The potential and current records obtained on immersing samples of the AA5083 in solutions of 3.5% NaCl, for variable periods of time, are presented and discussed. In accordance with an earlier study by Aballe, et al.,<sup>18</sup> this alloy undergoes two simultaneous corrosive processes, the relative importance of each depending on the length of time immersed. The first of these processes is related to the emergence of localized alkaline corrosion (LAC) phenomena at particular points on the surface of the samples. These processes have been related to the local increase of pH that is produced around the cathodic precipitates; this pH increase translates into the alkaline corrosion of the zones of the matrix that surround these precipitates.<sup>19,20</sup> This type of corrosion causes the loss of contact between the matrix and the cathodic precipitates, resulting in the physical detachment of the precipitates. The longer the period of immersion, the fewer precipitates remain exposed; consequently, the intensity of this corrosion process diminishes with time.<sup>19,21-22</sup> In parallel, the rest of the surface exposed is subjected to the growth of an anodic layer, the thickness of which increases with time of exposure.<sup>19,21</sup>

Figures 11 and 12, respectively, present records of potential ( $E$ ) and current ( $I$ ) corresponding to samples of AA5083 immersed in solutions of 3.5% NaCl for the periods of time indicated. It can be observed in these figures that, after the first hour of exposure, the  $E$  and  $I$  records are characterized by a large number of high-amplitude fluctuations; these can be associated with the first stages of the process of localized alkaline corrosion. As the time of exposure increases, a decrease in the number of these fluctuations is observed; this would coincide with the decreasing number of intermetallic particles exposed and, therefore, with a decrease in the intensity of the LAC process. For longer exposure times, the formation and dissolution of the layer of alumina becomes a process more active in the studied system. This latter process does not produce high-amplitude oscillations in the  $E$  and  $I$  signals (Figures 11 and 12). Therefore, the signal of the system studied can be considered to be composed of two components. The first of these is produced as a consequence of the LAC processes, while the second signal is due to the phenomena of the restructuring of the anodic layer. These two components that comprise each signal take different relative weights along the exposure time. Thus, in short periods of exposure, the predominant signal is that caused by the LAC phenomena, while for longer exposure times, both the formation and dissolution of the anodic layer and LAC processes contribute to the signals.

<sup>†</sup> Trade name.



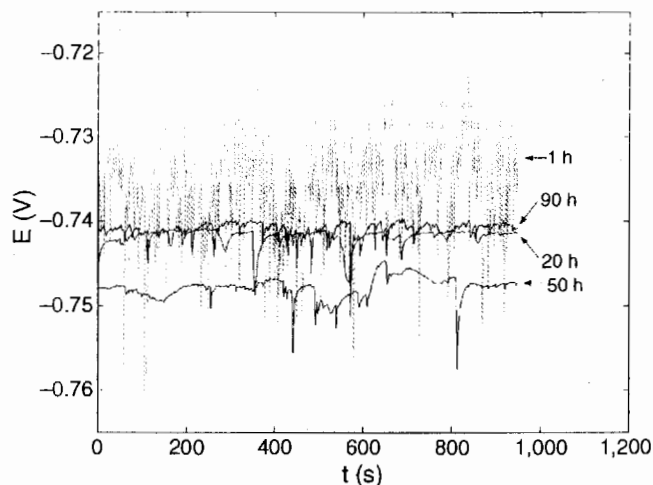


FIGURE 11. Examples of potential records of the AA5083 immersed in solutions of 3.5% NaCl for the periods of time indicated.

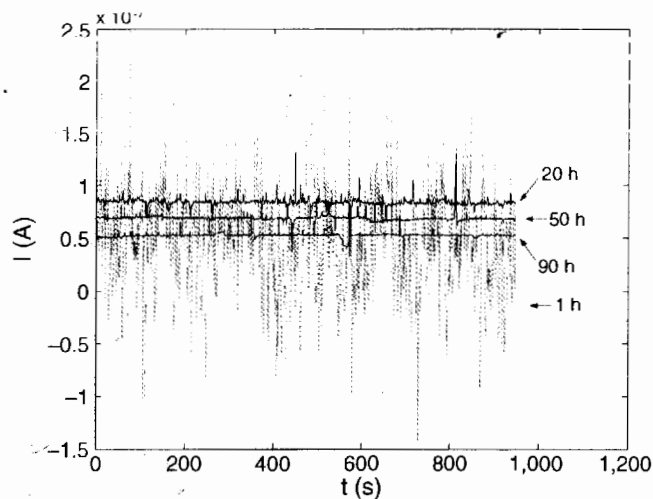
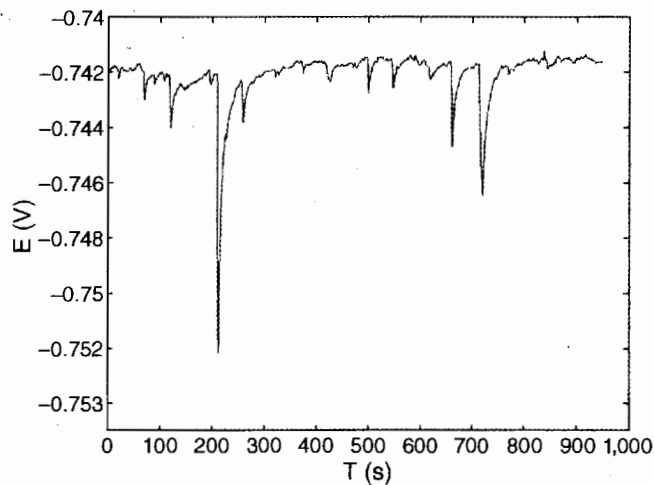


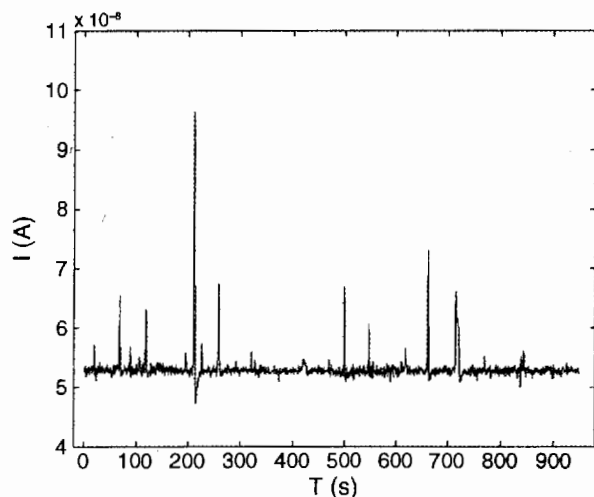
FIGURE 12. Examples of current records of the AA5083 immersed in solutions of 3.5% NaCl for the periods of time indicated.

In Figure 13, the records of  $E$  and  $I$  obtained after 90 h of immersion are presented. It can be seen in these figures that, for prolonged exposure times, high-amplitude oscillations continue to appear but are much more widely spaced compared to short exposure times (Figures 11 and 12). The spacing of these oscillations is associated with the decrease in the intensity of the LAC process. In Figure 14, the records presented in Figure 13 have been magnified, and the presence of the oscillations of low amplitude can be observed; these are associated with the phenomena of growth and subsequent dissolution of the anodic layer. It should be noted that these phenomena of growth and dissolution of the anodic layer are not reflected equally in the records of potential and current. So, although these signals are measured in different units and their appearance in the plots depends on the scale used, it seems that the current signals show fast fluctuations, while potential does not. It will be shown later that this feature reflects in the  $H$  values, and are a result of the formation and dissolution of the anodic layer.

Figure 15 gives the values of  $H$ , calculated for values of  $j$  between 16 and 512, from the R/S analysis of signals of  $E$  and  $I$  of AA5083 in NaCl solutions. These  $H$  values should be taken as a first approximation of analysis, especially when antipersistent signals are being studied, since these signals show a change in the slope. So, particular care should be taken when estimating the slope of R/S values of the antipersistent signals, since  $H$  will strongly change in the function of the interval of  $j$  taken for calculating the slope (Figures 5 through 9). As a consequence, calculating the slope between these values of  $j$  (16 and 512) is strictly suitable for random and persistent signals. In this Figure 15, it can be observed that, for times of exposures less than 20 h,  $H$  values are less than 0.5.



(a)



(b)

FIGURE 13.  $E$  and  $I$  records of AA5083/NaCl after 90 h of immersion.



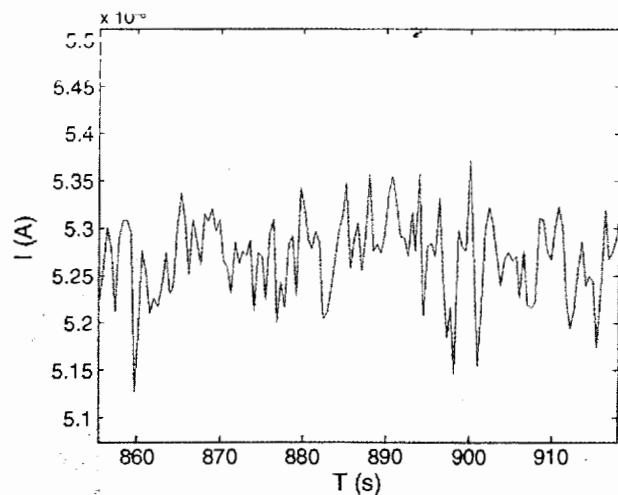
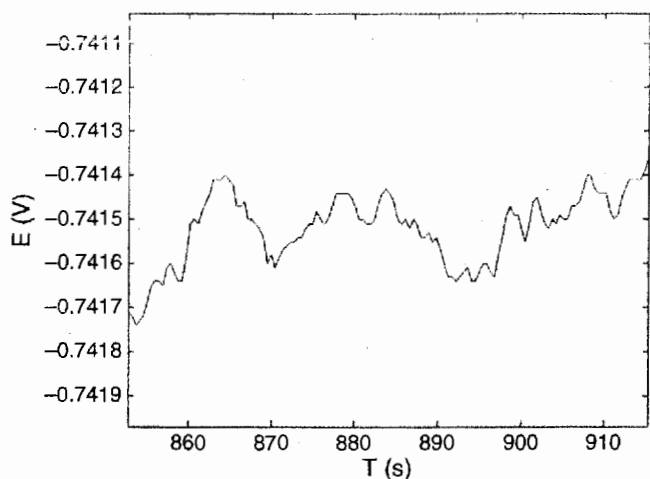


FIGURE 14. Magnification of the  $E$  and  $I$  records of AA5083/NaCl included in Figure 13.

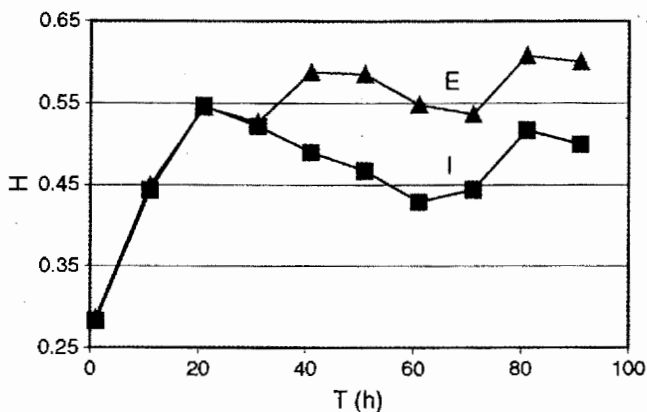


FIGURE 15.  $H$  values (taken in the range  $j \in [16, 512]$ ) of the  $E$  and  $I$  signals of AA5083 samples immersed in 3.5% NaCl, in the function of exposure time.

These  $H$  values suggest that the system is antipersistent in this interval of time. According to Horváth and Schiller,<sup>12</sup> this characteristic tells us that the occurrence of an event in the series analyzed delays the initiation of a new event. This explanation can be confirmed by observing the record of potential included in Figure 11. In effect, the emergence of a transient, associated with an event of localized corrosion, causes a decrease of the potential. This potential decrease delays the development of new pits until the potential values recover.

At short exposure times ( $< 20$  h), the dominant mechanism is pitting, a phenomenon that provokes the appearance of transients in potential and current records. The existence of so many transients in Figure 11 is from the very short constant time of these transients. The low constant time of the transient is caused by the high activity of the AA5083 surface,

since at this period of the immersion, no anodic layer is formed yet. So, for low immersion times, the signals are antipersistent, and  $H < 0.5$ . The developed pits provoke the delay of new pits, since a pit does not appear until the potential is recovered. However, there are many pits, because the potential recovery is rapid.

For longer exposure times, values of  $H > 0.5$  were observed in Figure 15, but this  $H$  has been estimated in the range of  $j$  between 16 and 512. This interval is able to detect the antipersistence of the signal, because the change in the slope takes place at high  $j$  ( $\tau_c > 256$ ). As was discussed, Figure 15 should be taken as a first approximation, especially in the study of antipersistent signals, which is the case.

As has been observed in the section of simulated signals, some signals show a  $\tau_c$  that indicates the scale in which the signal becomes antipersistent. To calculate  $\tau_c$  in the EN signals, a further investigation was performed using  $\text{Log } R/S$  vs.  $\text{Log } \tau$  and  $H_m$  vs.  $p$  plots.

In Figures 16 and 17,  $\text{Log } R/S$  vs.  $\text{Log } j$  values of AA5083 voltage signals immersed in NaCl have been included. The exposure time are indicated in these figures. Each  $R/S$  value included in these figures was obtained through averaging the  $R/S$  values of 10 records to obtain reliable results. In Figures 16 and 17, it can be seen that the slopes of these signals change with  $\tau$ . In addition, it can be observed that these variations in the slopes are smooth so it is difficult to estimate the  $\tau_c$  directly from these figures. To calculate this parameter, in Figures 18 and 19,  $H_m(p)$  values of the same signals plotted in Figures 16 and 17 have been included. In Figures 18 and 19, values of  $\tau_c = 32\Delta t$  were obtained for both potential and current signals obtained in the first hour of exposure. When Figures 11 and 12 are analyzed, it can be seen that the intervals between transients are lower than  $32\Delta t$ .

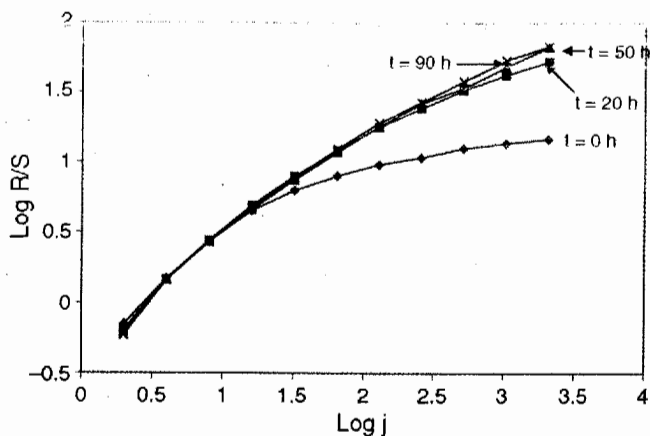


FIGURE 16. Values of  $\text{Log } R/S$  vs.  $\text{Log } j$  of E records of AA5083/NaCl after the exposure time indicated in the figure.

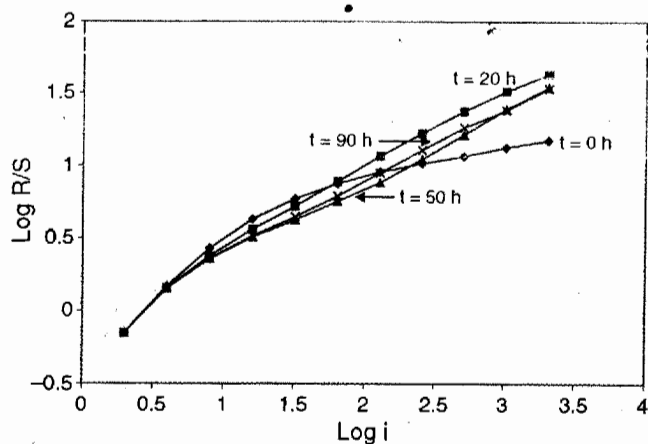


FIGURE 17. Values of  $\text{Log } R/S$  vs.  $\text{Log } j$  of I records of AA5083/NaCl after the exposure time indicated in the figure.

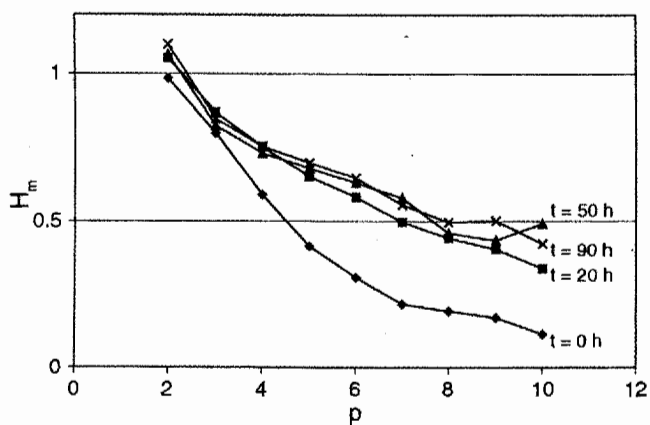


FIGURE 18. Values of  $H_m$  vs.  $p$  of E records of AA5083/NaCl after the exposure time indicated in the figure.

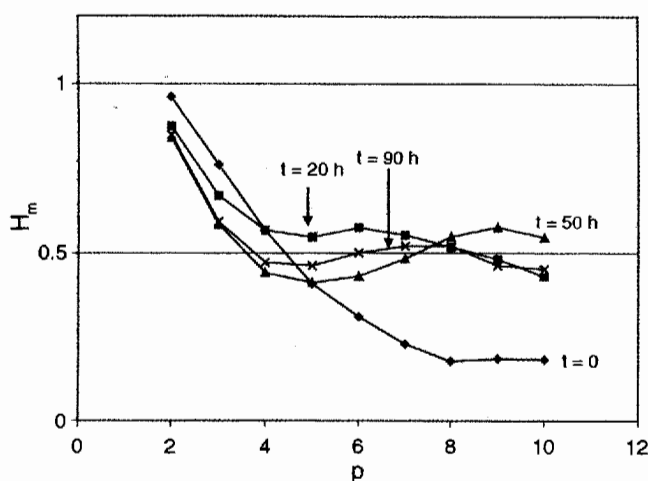


FIGURE 19. Values of  $H_m$  vs.  $p$  of I records of AA5083/NaCl after the exposure time indicated in the figure.

The R/S method does not accurately quantify the time between these overlapped transients. However, visual inspection of temporal records suggested that the obtained  $\tau_c$  could be taken as an approximation to the maximum distance between transients (single and overlapped transients). Therefore, an improved version of this method should be developed to accurately estimate the time between transients that overlap.

On the other hand, it can be appreciated in Figures 18 and 19 that for large exposure times (50 h or 90 h), the behavior of  $H_m$  is different for current and potential signals. Figure 18 shows that  $\tau_c$  values of these signals are higher than those measured in short exposure times. In fact,  $\tau_c = 256\Delta t$  for 50 h and 90 h of exposure, while  $\tau_c = 32\Delta t$  for 1 h of immersion. As was discussed, a low number of transients due to LAC processes had been observed for large periods of immersion (50 h to 90 h). Therefore, it can be deduced that the increase in the  $\tau_c$  values with the time of exposure is caused by the decrease in the activity of LAC.

In Figure 19, it can be seen that  $\tau_c = 16\Delta t$  for current signals obtained for large exposure times, while for potential signals (Figure 18),  $\tau_c = 256\Delta t$ . This feature can be due to the different fluctuations of potential and current associated with the restructuring of the anodic layer. So, in Figure 14, it can be appreciated that the current signal shows fluctuations of high frequencies and low amplitudes, which are thought to be reflected in the low value of  $\tau_c = 16\Delta t$ . In Figure 19, it is observed that in the current signal obtained after 90 h of immersion,  $H_m(p=4) < 0.5$ ,  $H_m(p=7)$  increases its value above 0.5 and finally  $H_m(p=9) < 0.5$ . Therefore, two values of  $\tau_c$  can be observed. The reason for the appearance of these two  $\tau_c$  values ( $\tau_{c,1}$  and  $\tau_{c,2}$ ) could be that the fluctuations of the signal due to the formation/dissolution of the anodic layer have similar importance to the fluctuations due to LAC processes. So, the first  $\tau_c$  ( $\tau_{c,1} = 16\Delta t$ ) can reflect the oscillations of high frequencies and low

amplitudes corresponding to the restructuring of the anodic layer, while the second  $\tau_c$  ( $\tau_{c,2} = 512\Delta t$ ) can be associated with the transients provoked by LAC processes.

## CONCLUSIONS

❖ EN signals of potential and current obtained after different times of exposure of AA5083 samples immersed in solutions of 3.5% NaCl have been analyzed in this study. The mathematical tool used to study these current and potential signals was the R/S method, which permits the classic Hurst exponent (H) of these series to be calculated. According to the literature, H can be obtained by means of estimating the slope of  $\log R/S$  vs.  $\log \tau$ . In the present paper, simulated and experimental EN signals did not give a constant slope of  $\log R/S$  vs.  $\log \tau$ , with H being dependent on the  $\tau$  values taken. In this paper, a new method for calculating H has been proposed. This methodology first uses the R/S method to calculate R/S(j) values, and second, estimates H for each  $\tau$  instead of calculating H for the whole series. The EN signals studied here showed antipersistence at different scales. The proposed method allows one to detect  $\tau_c$  of the signals; that is, the  $\tau$  where the signals become antipersistent.

❖ The results obtained have enabled the values of the Hurst exponent to be correlated with the mechanism of corrosion predominant in the different periods of immersion. So, the records of E and I taken in the first hours of immersion are characterized by many high-amplitude fluctuations, which can be associated with LAC. These records show overlapped transients, leading to  $\tau_c = 32\Delta t$ . Although the R/S method did not accurately quantify the time between these overlapped transients, visual inspection of temporal records suggested that  $\tau_c$  could be related to the maximum distance between transients. An improved method should be developed to accurately estimate the time between transients that overlap.

❖ On the other hand, for longer exposure times, the formation and dissolution of the layer of alumina becomes important. Current noise in this period of time was able to detect two values of  $\tau_c$ , one of them from

the fluctuations that provoke growth/renovation of the anodic layer ( $\tau_{c,1} = 16\Delta t$ ), and the second  $\tau_c$  ( $\tau_{c,2} = 512\Delta t$ ) from the contribution to the signal of the transients of LAC processes.

❖ This study suggests that a new Hurst exponent can be utilized as a tool that is sensitive to the changes taking place in the mechanism of corrosion for this type of system.

## ACKNOWLEDGEMENTS

This work has been financed by the Interministerial Commission for Science and Technology of Spain, the Junta de Andalucía, the project MAT2001-3477, and the project PETRI PTR1995-0836-OP.

## REFERENCES

1. H.E. Hurst, *Trans. Am. Soc. Civ. Eng.* 116 (1951): p. 770.
2. H.E. Hurst, *Nature*, 180 (1957): p. 494.
3. H.E. Hurst, R.P. Black, Y.M. Simaika, *Long-Term Storage, an Experimental Study* (London, U.K.: Constable and Co., 1965).
4. B. Mandelbrot, J.R. Wallis, *Water Resour. Res.* 5 (1969): p. 228.
5. B. Mandelbrot, J.R. Wallis, *Water Resour. Res.* 5 (1969): p. 967.
6. R.W. Komim, *Sol. Phys.* 156 (1995): p. 17.
7. R. Oliver, J.L. Ballester, *Sol. Phys.* 169 (1996): p. 216.
8. I. Simonsen, *Phys. A* 322 (2003): p. 597.
9. K. Chen, C. Jayaprakash, *Phys. A* 324 (2003): p. 258.
10. I.A. Lebedec, B.G. Shaikhatdenov, *J. Phys. G: Nucl. Part. Phys.* 23 (1997): p. 637.
11. M.A.F. Gomes, F.A. Souza, V.P. Brito, *J. Phys. D., Appl. Phys.* 31 (1998): p. 3,223.
12. Á. Horváth, R. Schiller, *Corros. Sci.* 45 (2003): p. 597.
13. G.N. Frantziskonis, L.B. Simon, J. Woo, T.E. Matikas, *Eur. J. Mech. A Solids* 19 (2000): p. 309.
14. M. Moon, B. Skerry, *J. Coat. Technol.* 67 (1995): p. 35.
15. H. Greisiger, T. Schauer, *Prog. Org. Coat.* 39 (2000): p. 31.
16. J.M. Sánchez-Amaya, J. Botana, M. Bethencourt, M.J. Cano, R.M. Osuna, "Study of the Methods of Calculating Hurst Exponent to be Applied to Corrosion Field," *Proc. EUROCORR 2004*, paper no. 455 (Nice, France: 2004), p. 1.
17. A. Aballe, "Advances in the Evaluation of Corrosive Processes by Means of Electrochemical Noise Application of Wavelets" (Ph.D. thesis, Puerto Real, Cadiz, Spain, 2001).
18. A. Aballe, M. Bethencourt, F.J. Botana, M. Marcos, J.M. Sánchez-Amaya, *Electrochim. Acta* 46 (2001): p. 2,353.
19. A. Aballe, M. Bethencourt, F.J. Botana, M.J. Cano, M. Marcos, *Corros. Sci.* 43 (2001): p. 1,657.
20. M. Bethencourt, F.J. Botana, M.J. Cano, M. Marcos, *Corros. Sci.* 45 (2003): p. 161.
21. A. Aballe, M. Bethencourt, F.J. Botana, M. Marcos, R. Osuna, *Mater. Corros.* 52 (2001): p. 185.
22. A. Aballe, M. Bethencourt, F.J. Botana, M.J. Cano, M. Marcos, "On the Reproducibility of the Electrochemical Response of AA5083 Alloy in NaCl Solutions," *Electrochemical Society Proceedings*, vol. 23 (Phoenix, AZ: 2000), p. 364.